OPTICAL NON-INVASIVE EVALUATION OF FERROELECTRIC FILMS/MEMORY CAPACITORS, **Sarita Thakoor, A. P. Thakoor, Jet Propulsion Laboratory, California Institute of Technology, Pasadena, California 91109 and L. Eric Cross, Pennsylvania State University, Materials Research Laboratory, University Park, PA**

NON-INVASIVE photoresponse (photocurrent/voltage , reflectance, and transmittance) from ferroelectric thin films and memory capacitors, with its strong dependence not only on the remanent polarization, but also on the film microstructure, crystal orientation, and nature of the interfaces (state of formation/ degradation, etc.) offers an excellent "tool" for probing the ferroelectric capacitors at virtually any stage of fabrication, including on-line quality control. In fact, simultaneous measurement of spectral photoresponse and spectral. reflectance, as a distinctive signature of the device probed, is an ideal, high speed, non-invasive means of evaluation for such thin films at high spatial resolution (~100 nm) using beam scanning. This paper discusses three aspects of such evaluation. First, the spectral transmittance of the film as a direct function of the microstructure, second, the use of band-gap illumination (365 nm) to condition a fatigued capacitor and , third, the high optical E field interaction with the ferroelectric capacitor, yields a high speed photoresponse which is directly related to the remanent polarization and the operational history(status of internal fields) of the ferroelectric capacitor. Combined, these different kinds of photoresponses provide a good signature of the device quality.

INTRODUCTION

Non-volatile ferroelectric memories are now in the advanced stages of development where issues such as high-yield manufacturability and long-term reliability are receiving increasing attention today. The leading implementation scheme[1-4] selected for the **VLSI** ferro-memories is based on remanent polarization within a ferroelectric capacitor, where the high speed switching of the polarization state provides a memory readout.

The performance characteristics (such as fatigue: loss of polarizability with read-write cycling, and memory retention issues- (a) aging: logarithmic decay of remanent polarization with storage time (b) imprint: the tendency of polarization to gradually return to a previously written state leading to bit error) of ferroelectric memory capacitors are governed by parameters such as:

* stability of the electrode/ferroelectric interfaces,
* orientation/epitaxy/crystallization status of the ferroelectric film,
* microstructure of the film: compactness, void density, surface smoothness, grain size, etc. and
* operational history.

Although all such critical parameters listed above are typically attempted to be well-controlled during the fabrication of

the memories, there is no suitable "tool" to conveniently and non-destructively "probe" the memory cells (during or after fabrication), with high spatial resolution and at high speed, for their polarization behavior which in effect dictates their ultimate performance with respect to fatigue, lifetime, imprint, etc. These problems are suspected to be originating due to the following causes:

(a) charged mobile defects (such as oxygen vacancies),

(b) existence of a-axis inclusions/ 90° domain walls,

(c) charge injection from the electrodes into traps in the ferroelectric material, and

(d) polarization of slow moving dipoles.

Particularly fatigue is suspected to occcur because of the screening of the applied voltage/pinning of domains by the accumulated space charge/defects/traps. In the recent past, significant strides have been made to address the issue of fatigue with the advent of new fatigue free "Y1" material and oxide/perovskite electrodes that provide a more stable chemical/structural template for the growth of the ferroelectric thin film. Long term retention problems such as imprint, however, continue to be a major reliability impediment

NON-INVASIVE photoresponse (photocurrent/voltage, reflectance and transmittance from ferroelectric thin films " and memory capacitors[6-14], with its strong dependence not only on the remanent polarization, but also on the film microstructure, crystal orientation, and nature of the interfaces (state of formation / degradation, etc) offers[15] just such an ideal "tool" for probing the

ferroelectric capacitors at virtually any stage of fabrication, including on-line quality control. In fact, simultaneous measurement of spectral. photoresponse and spectral reflectance, as a distinct signature of the device probed, is an ideal, high speed, non-invasive means of evaluation for such thin films at high spatial resolution (" 100 nm) using beam scanning. This paper discusses three aspects of such evaluation of ferroelectric lead zirconate titanate (PZT) thin films. First, the spectral transmittance of the film as a direct function of the microstructure, second, the use of band gap illumination (365 nm) to condition a fatigued capacitor and, third, the high optical E field interaction with the ferroelectric capacitor using pulsed lasers at 532 nm, yielding a high speed photoresponse which is directly related to the remanent polarization and the operational history (status of the internal fields) of the ferroelectric capacitor. This high speed photoresponse promises to be an unique non-invasive measure of the internal fields in the ferroelectric device as a evolving function of operation history, storage time and environmental history. Combined, these different kinds of photoresponses provide a good signature of the device quality.

EXPERIMENTAL DETAILS

PZT SPUTTER DEPOSITION

The **PZT** films were deposited by multi-target de-reactive sputtering of lead, zirconium, and titanium sequentially on a substrate rotating about the central axis of the chamber. The details of the chamber and sputtering process are discussed elsewhere[16]. A variety

of substrates, including borosilicate glass, quartz, iridium tin oxide(ITO) glass, sapphire and passivated silicon were used for the deposition. No intentional substrate heating was used. The temperature of the substrate during deposition was monitored using a thermocouple and was observed to stay below 60°C. The sputtering was carried out in a reactive gas mixture of high purity (99.999%) argon(inert gas) and oxygen(reactive gas) . The flow rates of Ar and O_2 were independently controlled by their respective flowmeters. The deposition routine typically consists of setting up the argon ambient and presputtering the targets to clean the surface. Next oxygen is added and the ambient stabilised. The target powers are set and the targets conditioned. Following this the shutter is removed and deposition is initiated on the rotating targets. Typical deposition conditions for obtaining film at the morphotropic phase boundary are as follows:

Background argon pressure, P_{Ar} = (8.0 - 8.5) mTorr
Sputtering pressure, $P_{Ar}+P_{O2}$ = (8.4 - 9.0)mTorr
Titanium sputter power . 60-75 watts'
Titanium sputtering current = 0.3A-0.35 A
Zirconium sputter power . 20-30 watts
Zirconium sputtering current = 0.15-0.2 A
Lead sputter power = 4.0 watts
Lead sputtering current = 0.05 A
Substrate to Target distance = 11.4 cm
Substrate rotation rate = 30-40 RPM
Deposition rates = 100-120 A/rein

As deposited the films were amorphous. The composite film so obtained was baked in an open air furnace at 525°C for one half hour or at 500°C for two hours after attaining steady temperature to yield the Zr rich rhombohedral phase. The surface topography of these films was studied using a Cambridge S250 Scanning Electron Microscope. The transmission response of these films in the spectral range of 200nm to 800 nm was observed using a Carey Model 5A Spectrophotometer.

SOL-GEL DEPOSITION:

The sol-gel lead zirconate titanate (PZT) thin films with a nominal composition of (Zr:52, Ti:48) were deposited by a modified Sayer's Technique[17,18] on oxidized silicon substrates covered with an evaporated Ti/Pt ("1000 Å/1000Å) base electrode. The lead zirconate titanate (PZT) film contained '18% excess lead and were '2000 Å thick. Crystallization of the as deposited PZT was accomplished by annealing the films at 550°C for 10 minutes in oxygen ambient. To complete a standard sandwich capacitor test structure-', semitransparent thin films of platinum (~ 150Å) were sputter-deposited as the top electrode. The top electrodes were patterned by conventional lift-off techniques as dots of 125pm and 250μm diameter. Optical transmission through the semitransparent top electrode films (λ = 300 to 800 nm) was about 30%.

BAND-GAP ILLUMINATION SET-UP:

Photonic probing at 365 nm was done using a short arc mercury

lamp as the near UV/visible (300nm to 600nm) illumination source with the strongest, line at 365nm isolated using a filter. The choice of this light source to obtain maximum photoresponse was motivated by the bandgap value of PZT ~3.5eV[10]. A custom built liquid light guide was utilized to deliver a 5mm divergent beam with an intensity of '0.1 watt/cm^2 onto the sample. A shutter controlled by a solenoid valve allowed a pulse illumination with a minimum pulse length of about 1 sec. The effect of this illumination on fatigued and unfatigued capacitors was observed. The details of the set-up utilized have been presented elsewhere[11,19]. The hysteris loops were all recorded at a 500 Hz frequency.

HIGH SPEED PHOTORESPONSE SET-UP:

The high speed photoresponse measurements were done using an energetic laser pulse that is capable of' heating the device. The doubled output at 532 nm from a Nd-YAG pulsed laser utilising accousto-optic switching was utilized for this experiments. The advantages of utilizing an accousto-optically switched laser over the electro-optically switched laser[6,8,9], in obtaining a low noise response signal. free from electromagnetic pickup of the high voltages (~ KV) used for electro-optic switching, have been illustrated elsewhere[12]. The incident photon energy was lower than the PZT bandgap (3.5 eV)[10], and was therefore weakly (c 1%) absorbed by the PZT. The laser pulse, has a full width at half maximum (FWHM) of ~ 1.0 ns and delivers power in the range of

$2mW/\mu m^2$ - 20 $mW/\mu m^2$ per pulse at 532 nm at a repeat frequency of 20 KHz. For the measurement of the photocurrent, the top and bottom electrodes of the ferro-capacitor were connected across the 50Ω internal impedance of an oscilloscope, which recorded the zero bias photoresponse from the capacitor on illumination with the laser pulse. The capacitor was poled positively by using a +4 V pulse for 1 msec or negatively by a -4 V pulse for the same duration.

RESULTS AND DISCUSSION :

SURFACE TOPOGRAPHY & OPTICAL TRANSMISSION CORRELATION:

The angle of incidence of the sputter deposit was a very critical parameter in determining the morphology and physical. characteristics of the films. Pig. la shows the Scanning Electron Microscope (SEM) picture of the surface of a film deposited in an unrestricted manner, allowing all angles of deposition. This film (type A film) was rough, opaque, and of ceramic quality. Fig. 1b shows the surface micrograph of a film obtained using identical deposition parameters, except a collimator around each gun restricted the deposition to a near-perpendicular incidence. Transparent electro-optic quality films (type B film) were obtained as a result of this restriction in the incidence angle of deposition. Devices made from films of type A were typically inferior in quality and had poor yield (more shorts or high leakage resistance) compared to those of type B.

Fig 2(a) and 2(b) are the transmission spectra for PZT with surface topographies corresponding to fig l(a) and 1 (b)

respectively. Therefore as is well-known, the transmission spectra serve as a simple screening tool for films with high surface roughness and high optical scattering from the films with good optical transmission quality.

EFFECT OF BAND-GAP LIGHT ILLUMINATION ON FERROELECTRIC MEMORY DEVICE :

Figure 3(a) shows the effect of band-gap light (365 nm) illumination on a fresh unfatigued ferroelectric memory capacitor. The dotted hysteresis loop is the one with no illumination and the solid line exhibits the hysteresis loop with illumination (10 sec pulse of 365 rim). It clearly shows that the 365 nm illumination causes the hysterisis loop to shift along the Y-axis and also there is a marked blooming of the hysteresis loop. Earlier [7-11] we have reported on the generation of a photovoltage/photocurrent due to such illumination for the duration of the light pulse. The figure 3(b) shows a similar comparison of the 'with' and 'without' illumination states of hysteresis loop for this memory capacitor fatigued to 10^8 cycles. However, in both these cases when the illumination was removed the hysteresis loops reverted back to their original unilluminated status. This suggests that the unfatigued capacitors and mildly fatigued capacitors primarily show only a reversible photoinduced change. Figure 4 illustrates the effect of the 365 nm illumination on the ferroelectric capacitor fatigued to 10^{10} cycles. Figure 4(a) is the loop for the fresh unfatigued capacitor, Fig 4(b) is the capacitor fatigued to 10^{10} cycles, Fig 4(c) is the loop just after turn-off of illumination

and figure 4(d) is the loop in the steady state 5 hours after turn-off. The temporal nature of the enhancement of the hysteresis loop in terms of remanent polarization suggests the existence of traps with different time constants. Progressively the cycling of the memory capacitor causes evolution of free space charge and defects that progressively fill up the trap sites. Illumination induced charge pairs could either recombine with the free space charge or cause emptying of the filled traps or cause both effects. The net result is to gives rise to the observed[7,10] steady photocurrent for the duration of the illumination. This leads to removal of the local screening fields due to the space charge and/or unpinning of domains pinned by the traps and hence a recovery of the fatigued state by regaining the loss of polarization. Similar observation of recovery from fatigue by UV illumination has been made by Warren et al[20] and Lee et al[21]. Additionally, figure 3 and 4 show that. fatigue causes an increase in the coercive voltage suggesting formation of a non-ferroelectric (resistive) interface/surface layer in the ferroelectric memory capacitor. It is interesting to note that the bandgap illumination either has no effect on the coercive voltage **or** in the fatigued cases causes a slight increase in the coercive voltage suggesting that the re-distribution of the charges could lead to a net increase of the resistive layer.

HIGH SPEED PHOTORESPONSE RESULTS :

A bipolar high speed photoresponse is obtained from freshly made capacitors for positive and negatively poled states respectively at

laser pulse power of $2mW/\mu m^2$ - 20 $mW/\mu m^2$. The unipolar response observed earlier[8] was specifi c to the LSCO\PZT\LSCO capacitors observed and was probably caused due to the presence of a rectifying junction in series with the ferroelectric capacitor. This was also evident in a marked shift of the hysteresis loops of those capacitors along the Y-axis such that it was located entirely in the negative quadrants. Figure 5 shows a comparison of the high speed photoresponse from the unfatigued and fatigued states of the memory capacitor (Pt/PZT/Pt) . The capacitance of the unfatigued state was 2.4 nF and the capacitance of the fatigued state was 1.3 nF. Figure 6 shows the corresponding hysteresis loops for the unfatigued and fatigued states of the memory respectively. The ratio of the unfatigued remanent polarization to the fatigued remanent polarization as determined from the hysteresis loops is identical to the ratio of the corresponding area under the peaks of the photoresponse signal for unfatigued and fatigued case. This clearly shows that the area under the photoresponse signal is proportional to the remanent polarization of the memory capacitor. Also the area under the photoresponse signal is interpreted[6,8-10] as being proportional to the ΔP, the net shift in the dipole moment due to the incidence of energetic laser pulse onto the capacitor. The area under the photoresponse peak therefore provides an excellent non-invasive, quantitative measure of remanent polarization. Also we observe that the speed of the photoresponse is directly dictated by the device capacitance and hence the photoresponse is expected to become faster with reducing ferroelectric pixel size, allowing very high speed non-invasive

measure of the memory state for the high density memories. The illumination pulse is non-invasive. The change AP is followed by an equivalent $-\Delta P$ so that that there is no net change in the remanent polarization, P_R as verified by *cross* checking using the conventional pulse switching measurement (DRO). Also, it was verified that the remanent polarization did no change for over 10^8 laser pulse readout cycles. Measurement of the photoresponse as a function of frequeny shows that the amplitude of the response saturates for frequencies lower than 10 Khz suggesting that the response attains its maximum value at ~100 μsec.

The mechanism[6,8] by which the shift ΔP occurs could be pyroelectric (thermally triggered, associated with temperature change within the PZT), piezoelectric (due to propagation through PZT of an acoustic deformation wave, initiated by a sudden thermal expansion of the platinum top electrode), or optical. rectification (due to interaction of the E-field associated with the incident photons and the internal fields within the ferroelectric. Experiments on twin capacitors to test the possibility of piezoelectric effect suggest that the piezoelectric contribution is relatively small.

Furthermore we find that the photoresponse has a dependence on the history of the memory capacitor. Fig 7 illustrates how the high speed photoeffect sensitively reflects the polarization history of the ferroelectric capacitor. A history has beeen induced in an accelerated mannerby applying a unidirectional

voltage for extended duration of 10 sec. The figure shows that the conventional pulse polarization destructive read-out (DRO) merely exhibits a slight asymmetry as a reflection of the history. In contrast, the high speed photoresponse shows an overall change from bipolar to unipolar response and therefore used directly for detecting the operational/environmental history of the ferroelectric memory **non-invasively**. This result may be of significant fundamental importance because it demonstrates that the photoresponse signal in addition to its dependence on remanent polarization is also dependent on the evolving internal fields within the ferroelectric (i.e. is the optical rectification effect) and thereby provides a measure of the internal screening fields within the ferroelectric. Such measure is not available as directly and non-invasively by conventional electrical techniques. The question now worth addressing is how these results could be extended to correlate the complex long term fatigue and retention effects with the photoresponse for reliability screening of such memories.

ACKNOWLEDGMENTS

Useful. discussions with Dr. Steve Bernacki on film deposition and Dr. Wayne Kinney and Dr. Dan Gealy on ferroelectric memories are gratefully acknowledged. Expert help from Dr. Hamid Hemmati and Mr John Michael Moorookian on the high speed photoresponse measurement set-up are gratefully acknowledged. Constant encouragement on this work and enlightening discussions with Dr. Terry Cole and Dr. Jim Cutts were invaluable. The work described in this paper was performed by the Jet Propulsion Laboratory, California Institute of Technology, and was sponsored in parts by the Advanced Research Projects Agency under an agreement with the National Aeronautics and Space Administration (NASA), JPL Director's Discretionary Fund and the NASA Office of Space Access and Technology.

REFERENCES:

1. W. Kinney, Integrated Ferroelectrics, 4(2), 131, (1994).
2. W. Kinney and F. D. Gealy, IEEE International Solid State Circuits Conference, p. 266, (1994).
3. J. T. Evans and R. Womack, An Experimental 51.2 bit Non-volatile Memory with Ferroelectric Storage Cell, IEEE Journal of Solid-State Circuits, 23, 1171-1176 (1988).
4. D. Bondurant and F. Gnandinger, Ferroelectric Non-volatile RAMs, IEEE Spectrum, 18, 30-33 (1989).
5. J. F. Scott and C. A. Paz De Araujo, Ferroelectric Memories, Science, 246, 1400-1405 (1989).

6. S. Thakoor, Appl. Phy. Lett. 60, 3319, 1992.

7. s. Thakoor, A.P. Thakoor, and S. E. Bernacki, Proc. Third international Symposium on Integrated Ferroelectrics, Pg. 262, April 3-5, 1991, Colorado Springs, Colorado.

8. S. Thakoor, Appl. Phy. Lett. 63, 3233, 1993.

9. S. Thakoor, Ferroelectrics, 134, 355, 1992.

10. S. Thakoor and J. Maserjian, "Photoresponse Probe of the space charge distribution in Ferroelectric PZT thin film memory capacitors" J. Vat. Sci. & Tech A, 12, 295, Mar/April (1994).

11. S. Thakoor, Journal of Appl. Physics, 75 (10), 5409, May 15 (1.994).

12. S. Thakoor, E. Olson and R. H. Nixon, "Optically Addressable Ferroelectric Memory and its Applications" Integrated Ferroelectrics", 4, 257 (1994) .

13. s. Thakoor and A. P. Thakoor, "Optically Addressed Ferroelectric Non-Volatile Memories", Proceedings of the 1994 Spring Conference on Solid-State Memory Technologies, p. 107, Pasadena May 23-25, 1994.

14. s. Thakoor, J. M. Morookian, H. Hemmati and A. P. Thakoor, International Symposium of Applied Ferroelectrics held August 7-1o, 1994 at Penn State Scanticon, State College, Pennsylvania. S. Thakoor, J. M. Morookian, H. Hemmati and A. P. Thakoor, " Low Noise Set-up for High Speed Photoresponse Measurement", JPL New Technology Report, November 1994.

15. S. Thakoor, New Technology Report # NPO - 19393/8994. S. Thakoor, *NASA TechBriefs*, Vol. 17, p. 54 May (1993) .

16. S.Thakoor, U. S. Patent # 5196101, March 23, 1993.

17. G. Yi, Z. Wu and M. Sayer, J. Appl. Phys. 64, 2717 (1988) .

18. S. E. Bernstein et al, Proc. MRS Fall Meeting: Symposium on Ferroelectric Thin Films II, Vol 243, p 343, Published by Materials Research Society, Pittsburgh, Pennsylvania, Boston, Dec 2-4 (1991).

19. M. Lakata, and S. Thakoor, "Automated Ferroelectric Capacitor Testing System", NASA Tech Briefs, 18, 30 (1994)15.

20. W. L. Warren, D. Dimes, B. A. Tuttle, R. D. Nasby, and G. E. Pike, (submitted Applied Physics Letters)

21. J. Lee, S. Esayan, A. Safari, and R. Ramesh, Appl. Phys. Lett. 64 3646 (1994).

JPL

SURFACETOPOGRAPHY OF SEQUENTIAL, REACTIVE, MAGNETRON, SPUTTER DEPOSITED PZT

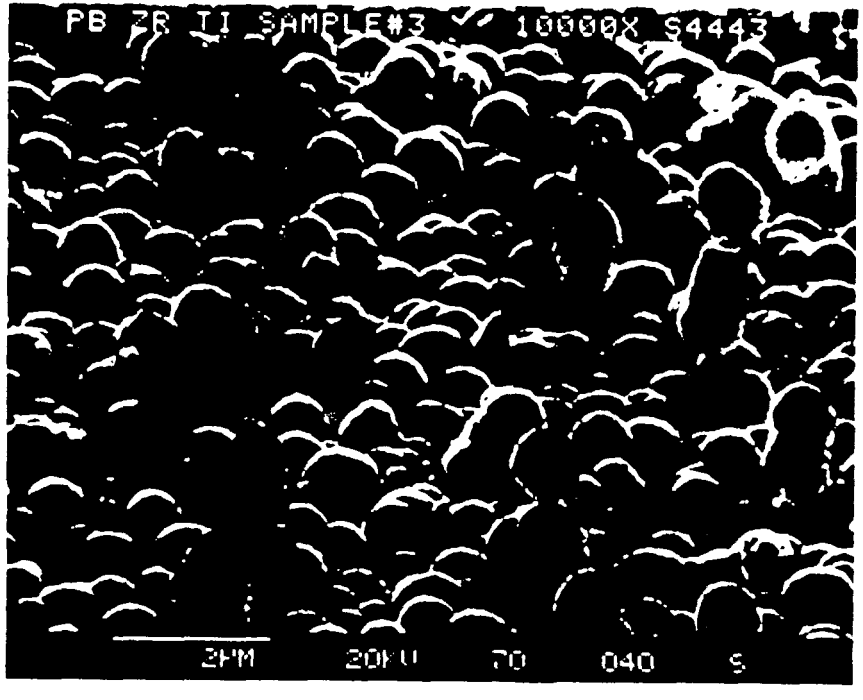

PZT: HIGH OPTICAL SCATTERING
SURFACE ROUGHNESS ~1μm

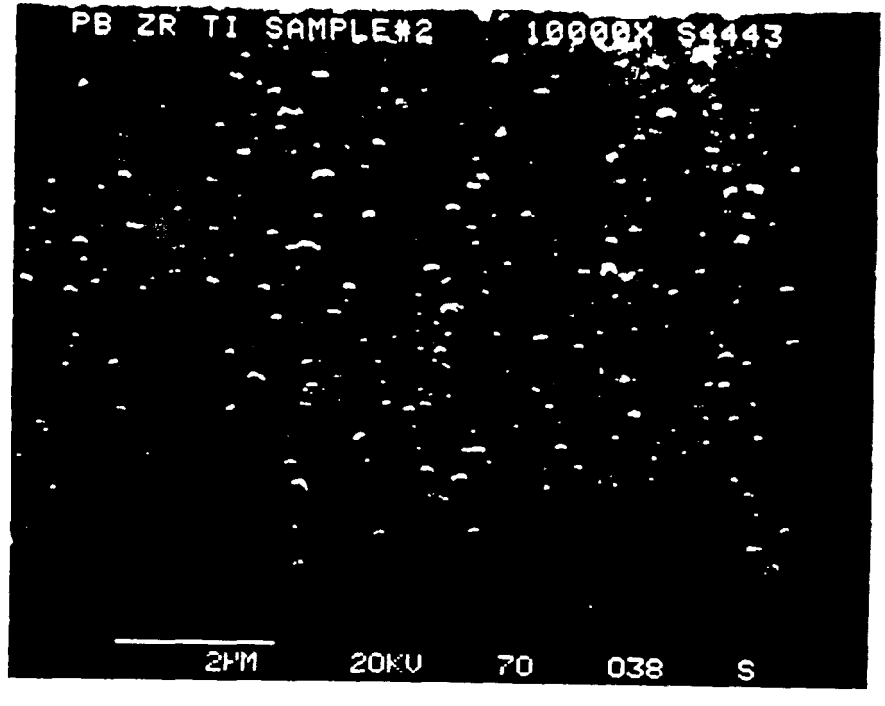

PZT: GOOD OPTICAL TRANSMITTANCE
SURFACE ROUGHNESS ~ 0.2μm

FIG 1

JPL

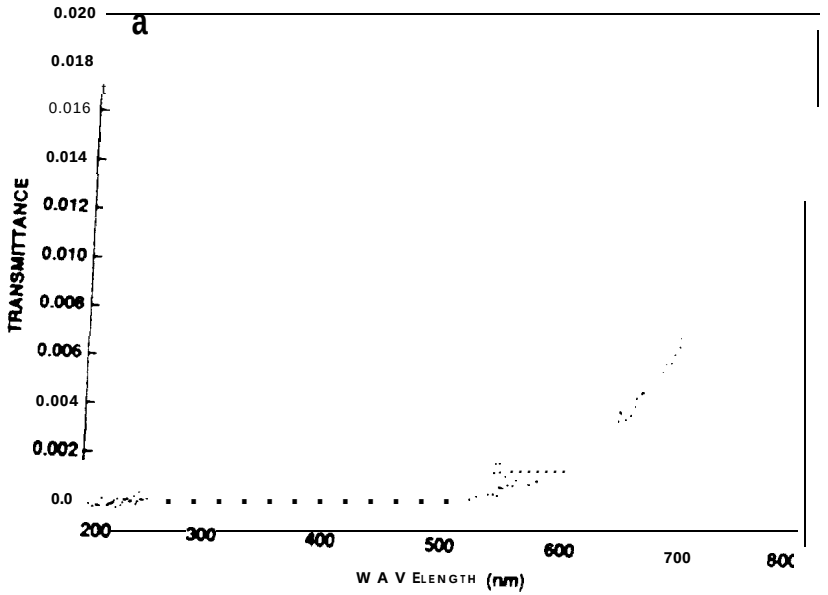

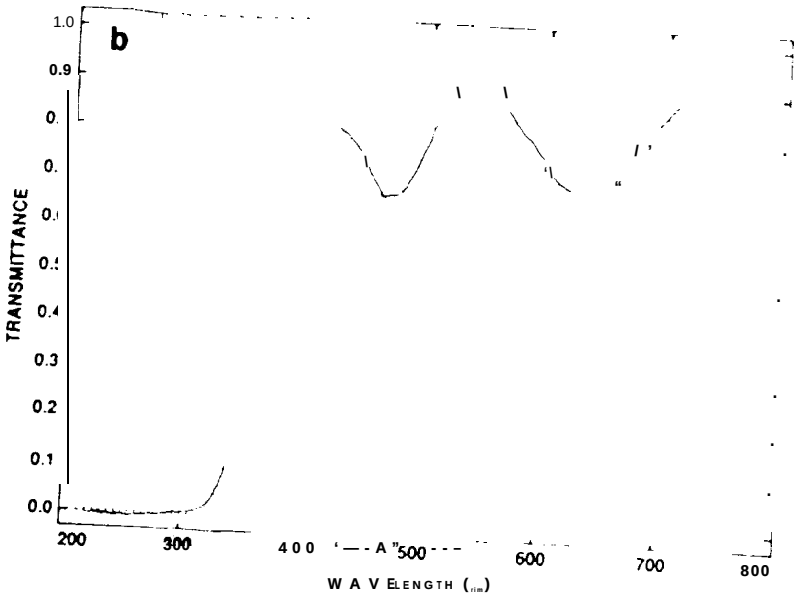

PZT: HIGH OPTICAL SCATTERING
SURFACE ROUGHNESS ~1μm

PZT: GOOD OPTICAL TRANSMITTANCE
SURFACE ROUGHNESS. 0.2μm

FIG 2

JPL

EFFECT OF BANDGAP ILLUMINATION COMPARISON UNFATIGUED AND FATIGUED STATE

a

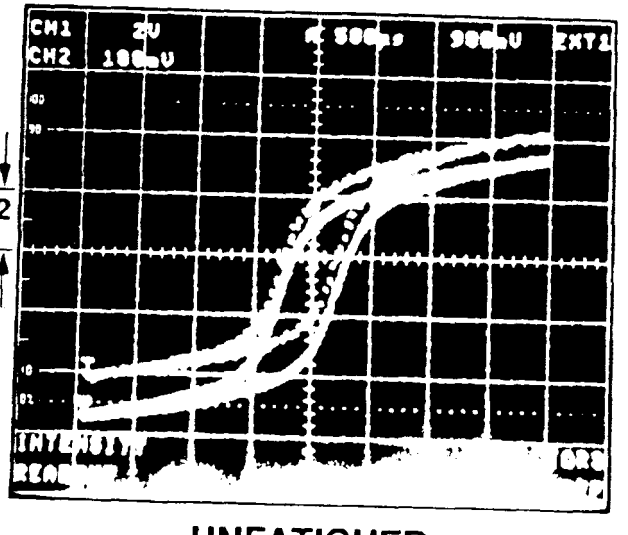

20 μC/cm^2

UNFATIGUED

b

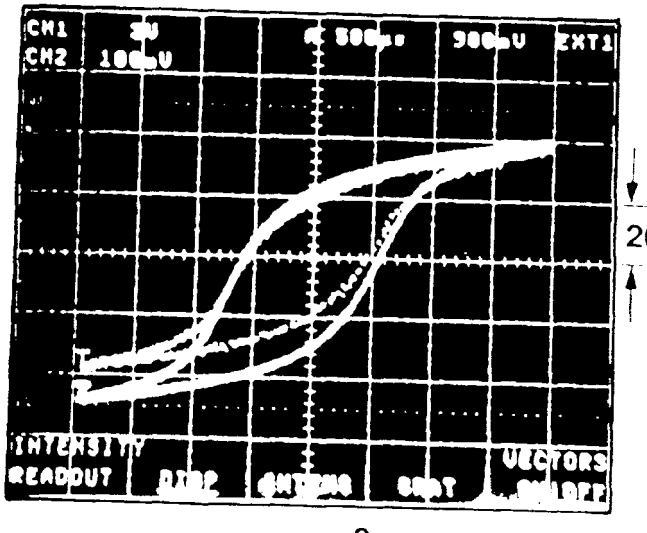

20 μC/cm^2

FATIGUED, 10^8 CYCLES

DOTTED LINE - WITHOUT ILLUMINATION
FULL LINE - WITH ILLUMINATION

FIG 3

JPL

EFFECT OF BANDGAP ILLUMINATION ON FATIGUED CAPACITOR

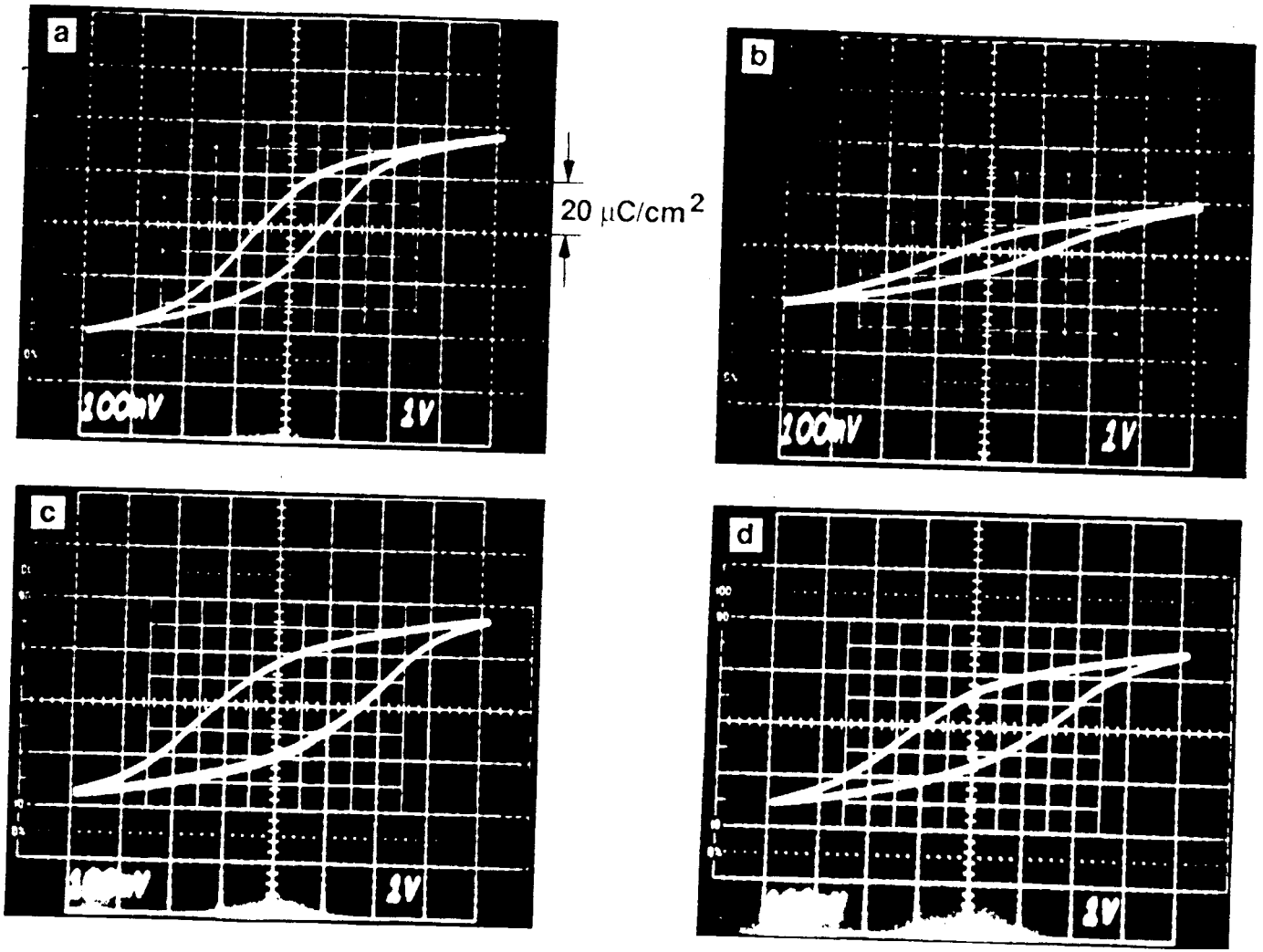

HYSTERESIS LOOPS AT 500 Hz: (a): INITIAL STATE (b) : FATIGUED STATE
(c) : ILLUMINATION REJUVENATED STATE, 1st LOOP AFTER ILLUMINATION TURN-OFF
(d) : ILLUMINATION OF REJUVENATED STATE, STEADY STATE LOOP AFTER ILLUMINATION TURN-OFF.

FIG. 4

JPL

HIGH SPEED PHOTORESPONSE:
UNFATIGUED INITIAL STATE

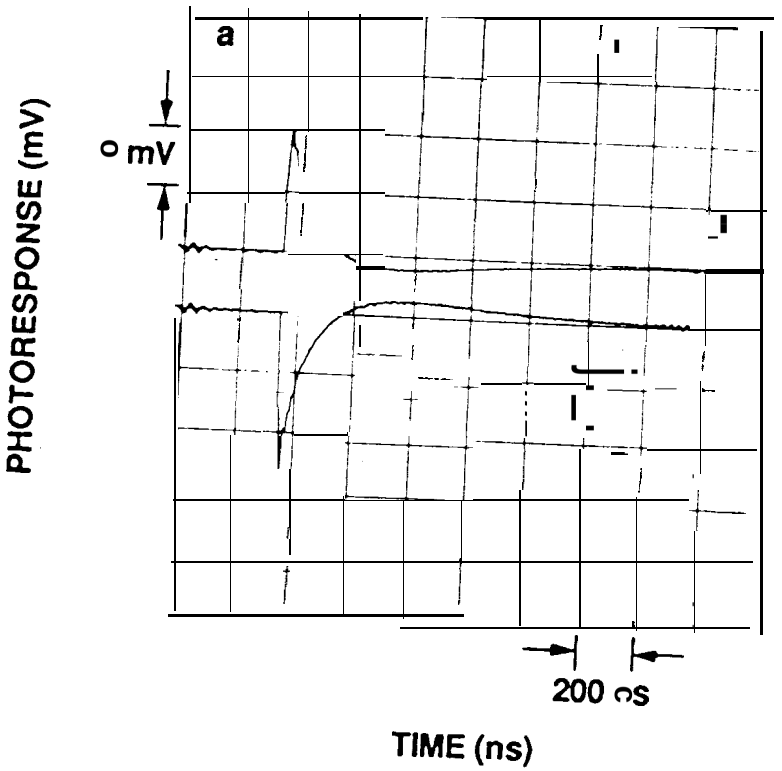

HIGH SPEED PHOTORESPONSE:
FATIGUED STATE

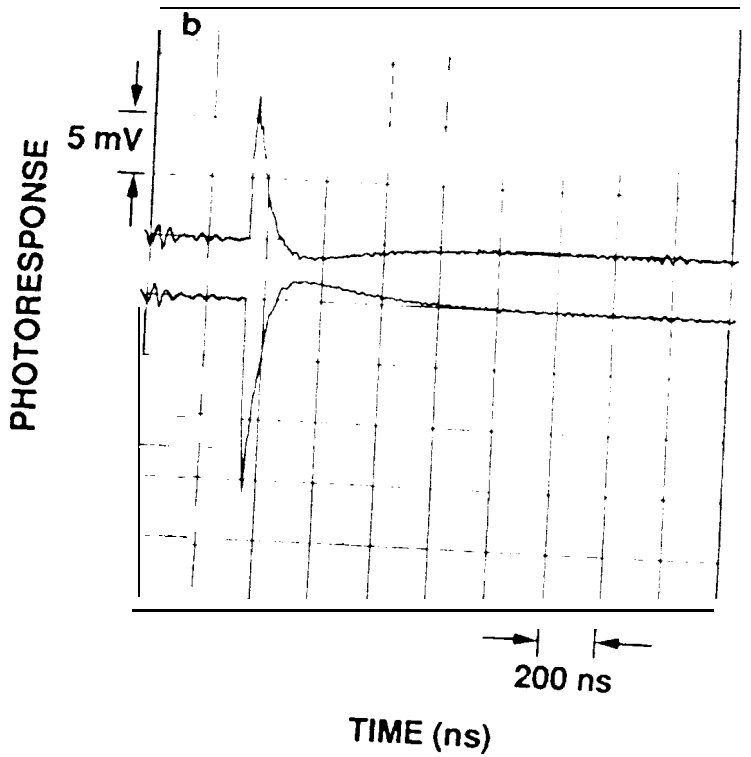

FIG 5

JPL

HYSTERESIS LOOPS (1 kHz) FATIGUED AND UNFATIGUED STATES COMPARISON

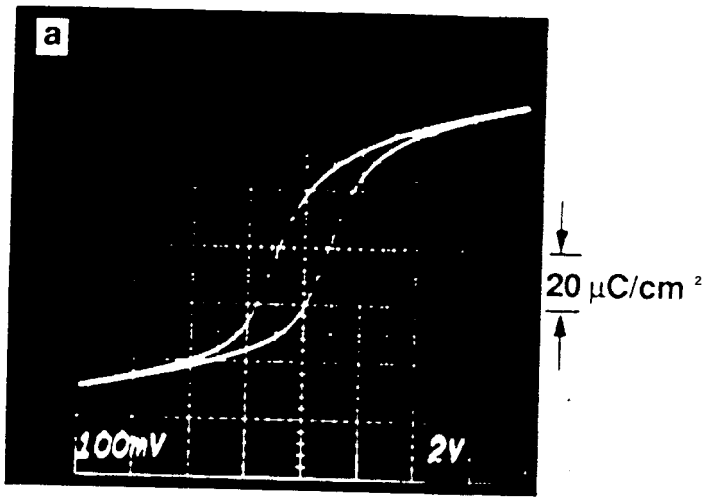

UNFATIGUED INITIAL STATE

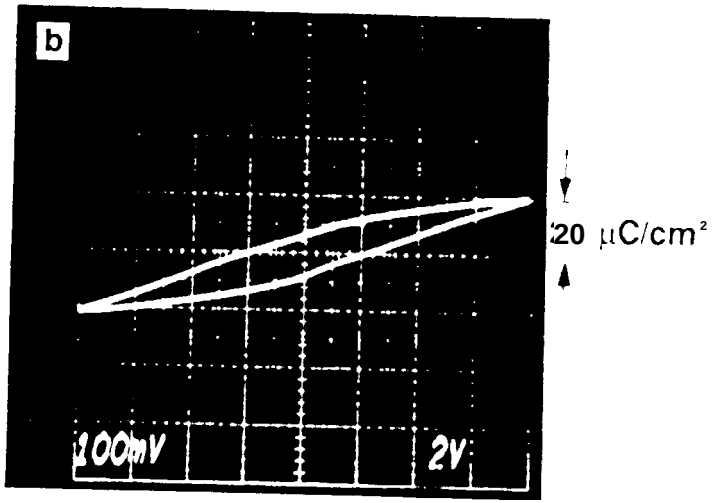

FATIGUED STATE (10^{10} CYCLES)

Fig 6

JPL PHOTORESPONSE: PROBING FOR "HISTORY" OF THE FERROELECTRIC CAPACITORS

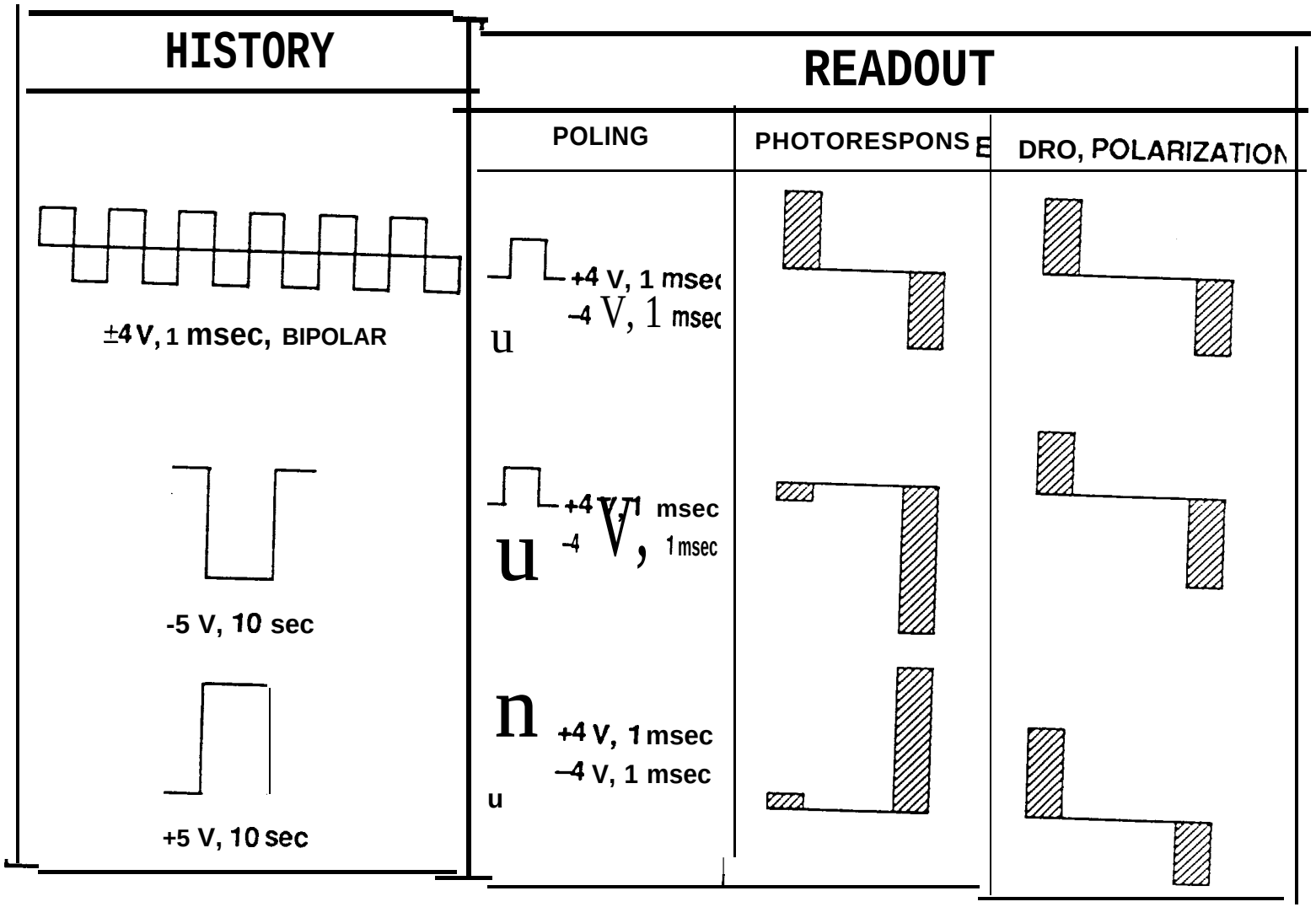

FIG 7

JPL

High Speed Photoresponse Analysis

Poling Polarity	Ratio: $\frac{\text{Unfatigued Polarization}}{\text{Fatigued Polarization}}$ determined by hysteresis loop	Ratio: $\frac{\text{Area under peak, unfatigued}}{\text{Area under peak, fatigued}}$ determined by photoresponse
positive	2.57	2.57
negative	2.62	2.65